THE ANNALS OF "DUNAREA DE JOS" UNIVERSITY OF GALATI
FASCICLE V, TECHNOLOGIES IN MACHINE BUILDING,
ISSN 2668-4829 (PRINT) 2668-4888 (ONLINE)
https://doi.org/10.35219/tmb.2025.1.12

ABSOLUTE/CONVECTIVE INSTABILITIES ANALYSIS IN A DOUBLE DIFFUSIVE ENVIRONMENT

Maria NEAGU [1]

[1] "Dunarea de Jos" University of Galati.
Manufacturing Engineering Department, Galaţi, Romania
email: maria.neagu@ugal.ro

ABSTRACT

This paper presents the instability analysis of the buoyancy layers that exists near a vertical impermeable wall of constant temperature and mass flux situated in a linearly mass stratified fluid (the Prandtl number Pr=6.7). The dimensionless parameter M=RaSc[Sch^(4/3)]/[(N^3)Pr(1+Pr)](where Ra is the Rayleigh number, Sch is the Smith number, N is the buoyancy ratio and Sc is the dimensionless mass stratification parameter) separates the two possible equilibrium situations: a heat driven convection (HDC) regime along the wall if M>1 and a HDC-MDC (mass driven convection) regimes succession if M<1.

Two particular parameter sets are considered for the two situations mentioned above: Case I [Ra=1.0x(10^11), N=1, Le=2, Pr=6.7, Sc=0.05] (HDC regime); Case II: [Ra=1.0x(10^11), N=3000, Le=5, Pr=6.7, Sc=0.04](HDC-MDC regime).

The HDC regime generated by the case I parameter set is convectively unstable, no matter where the instantaneous perturbation is applied, while an absolutely unstable situation appears for the HDC-MDC regime of case II when the perturbation is applied in the HDC region.

KEYWORDS: natural convection, stability, double diffusion

1. INTRODUCTION

The general problem of double diffusion natural convection process that occurs near a vertical wall situated in a fluid environment received great attention in the scientific literature due to its numerous practical applications.

Recently, this problem was studied for the particular case of a constant temperature and mass-flux wall embedded in a linearly mass-stratified environment [1-3]. These studies revealed the special importance of a certain parameter M that is defined as follows:

- if Pr<1, $M = Ra \cdot S_C \cdot Sch^m / \left[N^3 \, Pr(1+Pr)\right]$;

where $m = \begin{cases} 4/3 & if \quad Sch \geq 1 \\ 2 & if \quad Sch < 1 \end{cases}$;

- if Pr≥1, $M = Ra \cdot \gamma^2 \cdot S_C \cdot Le^{4/3} \cdot N^{-3}$,

where $\gamma = 1 - \left(1 + Pr^{1/2}\right)^{-1}$, Ra is the Rayleigh number, Pr is the Prandtl number, Sch is the Smith number, S_c is the mass dimensionless stratification of the environment and Le is the Lewis number.

A heat-driven convection (HDC) or a heat-mass-driven convection (HDC-MDC) regime succession reaches an equilibrium state along the wall if $M \geq 1$ or $M < 1$, respectively.

The consequences of the change in the natural convection process along the vertical impermeable wall were further studied for the particular case of $Pr = 0.72 < 1$ and $Sch \geq 1$ [4]. The stability analysis was performed for two particular parameter sets, $Ra = 5000, \quad N = 1, \quad Le = 1, \quad S_C = 0.08$ and $Ra = 5000, \quad N = 5, \quad Le = 1, \quad S_C = 0.04$, corresponding to the HDC and the HDC-MDC cases, respectively, and the results revealed that for both cases, a convectively unstable behaviour of the system occurs when perturbations are applied at the leading edge of the wall. Further, the analysis of the energy equilibrium of the perturbations' temperature, concentration, and stream function fields revealed that the nature of the natural convection process dictates significant differences in the evolution of the buoyancy, the transfer from the main stream, and the viscous dissipation contributions to the perturbations energy equilibrium.

This work extends the previous analyses by considering a higher value of the Rayleigh number, $Ra = 1.0 \times 10^{11}$, a value that allows us to compare the absolutely unstable and the convectively unstable domains. Two well-chosen parameter sets will allow us this comparison:

- Case I: $Ra = 1.0 \times 10^{11}$, $N = 1$, $Le = 2$, $Pr = 6.7$, $S_C = 0.05$ (the HDC regime) and
- Case II: $Ra = 1.0 \times 10^{11}$, $N = 3000$, $Le = 5$, $Pr = 6.7$, $S_C = 0.04$ (the HDC-MDC regime).

The analysis proceeds as follows:
- section 2 of the paper presents the mathematical model, the dimensional and the dimensionless governing equations, along with the corresponding boundary conditions;
- section 3 presents the scale analysis for the problem defined in this paper and it regains the formula for the parameter M;
- section 4 presents the conservation equations and the boundary conditions for the perturbation field;
- section 5, results and discussions, presents the temperature, the concentration, and the stream function fields for the two particular parameter sets considered in this paper; it shows the results of the simulation for two instantaneous perturbations applied at different abscissas along the wall and it underlines the main results of this analysis.

2. MATHEMATICAL MODEL

A vertical impermeable wall of constant temperature, T_w, is situated in a constant temperature, T_∞, environment. The mass flux of a certain constituent, q_w, is constant at the wall while the environment linear mass stratification parameter is s_C.

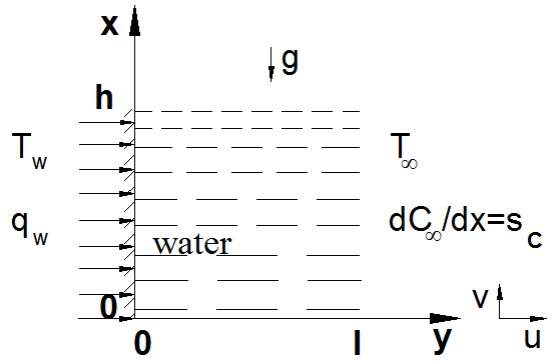

Fig. 1. *Computational domain*

Figure 1 presents the dimensional problem where the following notations were used: T − the temperature, C − the concentration, l and h − the right and the upper limit of the computational domain, respectively, u and v − the horizontal and the vertical velocities.

The dimensional mass, momentum and energy equations [1-3]:

$$\frac{\partial v}{\partial x} + \frac{\partial u}{\partial y} = 0 \quad (1)$$

$$\frac{\partial u}{\partial t} + u \cdot \frac{\partial u}{\partial y} + v \cdot \frac{\partial u}{\partial x} = -\frac{1}{\rho}\frac{\partial p}{\partial y} + \nu\left(\frac{\partial^2 u}{\partial x^2} + \frac{\partial^2 u}{\partial y^2}\right) \quad (2)$$

$$\frac{\partial v}{\partial t} + u \cdot \frac{\partial v}{\partial y} + v \cdot \frac{\partial v}{\partial x} = -\frac{1}{\rho}\frac{\partial p}{\partial x} + \nu\left(\frac{\partial^2 v}{\partial x^2} + \frac{\partial^2 v}{\partial y^2}\right) + \quad (3)$$
$$+ g\beta_t \Delta T + g\beta_c \Delta C$$

$$\frac{\partial T}{\partial t} + u \cdot \frac{\partial T}{\partial y} + v \cdot \frac{\partial T}{\partial x} = \alpha\left(\frac{\partial^2 T}{\partial x^2} + \frac{\partial^2 T}{\partial y^2}\right) \quad (4)$$

$$\frac{\partial C}{\partial t} + u \cdot \frac{\partial C}{\partial y} + v \cdot \frac{\partial C}{\partial x} = D\left(\frac{\partial^2 C}{\partial x^2} + \frac{\partial^2 C}{\partial y^2}\right) \quad (5)$$

require the associated boundary conditions [1-3]:

$$u = v = 0,\ T = T_w,\ \frac{\partial C}{\partial y} = -\frac{q_w}{D} = -\Gamma_w \text{ at } y = 0 \quad (6)$$

$$v = 0,\ T = T_{\infty,x},\ C = C_{\infty,x} \text{ as } y \to \infty \quad (7)$$

$$v = 0,\ T = T_{\infty,x},\ C = C_{\infty,x} \text{ at } x = 0 \quad (8)$$

$$\frac{\partial^2 u}{\partial x^2} = \frac{\partial^2 v}{\partial x^2} = \frac{\partial^2 T}{\partial x^2} = \frac{\partial^2 C}{\partial x^2} = 0 \text{ at } x = h, \quad (9)$$

where $\Delta T = T_w - T_\infty$ and $\Delta C = C - C_{\infty,x}$; t − the time, p − the pressure, α − the thermal diffusivity, D − the mass diffusivity and ν is the kinematics viscosity.

The following dimensionless variables will be used simultaneously with the dimensional variables for a better understanding of the analysis:

$$X = \frac{x}{L}Gr^{1/4};\ Y = \frac{y}{L}Gr^{1/4};$$
$$U = \frac{u \cdot L}{\alpha \cdot Gr^{1/2}}$$

$$\tau = \frac{t \cdot \alpha}{L^2} \cdot Gr^{3/4};\ \Psi = \frac{\omega}{Gr^{3/4}}\frac{L^2}{\alpha};$$

$$P = \frac{pL^2}{\rho\upsilon^2} \cdot \frac{1}{Gr};\ \theta = \frac{T - T_\infty}{T_w - T_\infty}, \quad (10)$$

where $S_C = s_C / \Gamma_w$ is the dimensionless mass stratification parameter, $Ra = \frac{g\beta_t L^3 \Delta T}{\alpha\nu}$ and the Grashof number $Gr = Ra / Pr$.

The dimensionless form of the conservation equations is

$$\frac{\partial V}{\partial X}+\frac{\partial U}{\partial Y}=0 \tag{11}$$

$$\frac{\partial U}{\partial \tau}+U\cdot\frac{\partial U}{\partial Y}+V\cdot\frac{\partial U}{\partial X}= =-Pr^2\cdot\frac{\partial P}{\partial Y}+\frac{Pr}{Gr^{1/4}}\cdot\left(\frac{\partial^2 U}{\partial X^2}+\frac{\partial^2 U}{\partial Y^2}\right) \tag{12}$$

$$\frac{\partial V}{\partial \tau}+U\cdot\frac{\partial V}{\partial Y}+V\cdot\frac{\partial V}{\partial X}=-Pr^2\cdot\frac{\partial P}{\partial X}+ +\frac{Pr}{Gr^{1/4}}\cdot\left(\frac{\partial^2 V}{\partial X^2}+\frac{\partial^2 V}{\partial Y^2}\right)+\frac{Pr^2}{Gr^{1/4}}\cdot(\theta+N\cdot\phi) \tag{13}$$

$$\frac{\partial \theta}{\partial \tau}+U\cdot\frac{\partial \theta}{\partial Y}+V\cdot\frac{\partial \theta}{\partial X}= =\frac{1}{Gr^{1/4}}\left(\frac{\partial^2 \theta}{\partial X^2}+\frac{\partial^2 \theta}{\partial Y^2}\right) \tag{14}$$

$$\frac{\partial \phi}{\partial \tau}+U\cdot\frac{\partial \phi}{\partial Y}+V\cdot\frac{\partial \phi}{\partial X}+V\cdot\frac{S_c}{Gr^{1/4}}= =\frac{1}{Le\cdot Gr^{1/4}}\left(\frac{\partial^2 \phi}{\partial X^2}+\frac{\partial^2 \phi}{\partial Y^2}\right) \tag{15}$$

Defining the horizontal and the vertical dimensionless velocities as $U=-\partial\Psi/\partial X$ and $V=\partial\Psi/\partial Y$, the dimensionless stream function formulation of the conservation equations (11) ÷ (13) becomes:

$$\zeta=\left(\frac{\partial^2 \Psi}{\partial Y^2}+\frac{\partial^2 \Psi}{\partial X^2}\right) \tag{16}$$

$$\frac{\partial \zeta}{\partial \tau}+U\frac{\partial \zeta}{\partial Y}+V\frac{\partial \zeta}{\partial X}=\frac{Pr}{Gr^{1/4}}\cdot\left(\frac{\partial^2 \zeta}{\partial Y^2}+\frac{\partial^2 \zeta}{\partial X^2}\right) +\frac{Pr^2}{Gr^{1/4}}\cdot\left(\frac{\partial \theta}{\partial Y}+N\frac{\partial \varphi}{\partial Y}\right) \tag{17}$$

The corresponding dimensionless boundary conditions are:

$$\Psi=\frac{\partial \Psi}{\partial Y}=0,\ \frac{\partial \varphi}{\partial Y}=-\frac{1}{Gr^{1/4}},\ \theta=1 \text{ at } Y=0 \tag{18}$$

$$\frac{\partial \Psi}{\partial Y}=0,\ \zeta=0,\ \theta=\varphi=0 \text{ as } Y=L \tag{19}$$

$$\Psi=0,\ \zeta=0,\ \theta=\varphi=0 \text{ at } X=0 \tag{20}$$

$$\frac{\partial^2 \psi}{\partial X^2}=\frac{\partial^3 \psi}{\partial X^3}=\frac{\partial^2 \theta}{\partial X^2}=\frac{\partial^2 \varphi}{\partial X^2}=0 \text{ at } X=H \tag{21}$$

The governing equations (14) ÷ (17) with the boundary conditions (18) ÷ (21) were solved using the finite differences method [1-3].

3. SCALE ANALYSIS

This section is divided as follows:

- the transient state, section 3.1;
- the heat driven convection (HDC) regime, section 3.2;
- the mass driven convection (MDC) regime, section 3.3.

3.1. Scale analysis of the transient state

In the beginning, the equilibrium of the inertia and the horizontal diffusion of heat characterises the equation (4): $\frac{\partial T}{\partial t}\sim\alpha\cdot\frac{\partial^2 T}{\partial y^2}$. For a temperature difference across the thermal boundary layer $\Delta T\sim T_w-T_\infty$, the temperature boundary layer thickness is [1]:

$$\delta_T\sim\alpha^{1/2}\cdot t^{1/2} \tag{22}$$

The equilibrium between the inertia and the horizontal diffusion of the species [1], in equation (5), $\frac{\partial C}{\partial t}\sim D\cdot\frac{\partial^2 C}{\partial y^2}$, gives us an estimate of both the concentration boundary layer thickness, δ_C:

$$\delta_C\sim D^{1/2}\cdot t^{1/2} \tag{23}$$

and the concentration difference across the boundary layer: $\Delta C\sim\Gamma_w D^{1/2}t^{1/2}$.

Two important observations we have to register at this point of the analysis:

1. As we can easily notice, because $Le=\alpha/D\geq 1$, in the beginning, the $\beta_t\Delta T$ term is much greater than the $\beta_c\Delta C$ across the boundary layers. This inequality signifies the presence of heat driven convection (HDC) regimes in every abscissa along the wall. The heat driven convection regime becomes a mass driven convection (MDC) regime depending on the process parameters and the abscissa.
2. The environment has a vertical variation of the specie concentration $\partial C/\partial x$ of value s_C. In the beginning the $\partial C/\partial x$ term in equation (5) has an order of magnitude of s_c in the boundary layer at any x co-ordinate. As the concentration boundary layer receives at any moment a mass flux, we cannot have in equation (5) a value of $\partial C/\partial x$ term smaller than s_C.

Having in view the two observations made above, Neagu [1] mentioned two moments of great interest in this analysis:

1. the time when the transition HDC→MDC transition might occur at an abscissa, t_{trz};
2. the time when the $\partial C/\partial x$ term in equation (5) increases so much that its order of magnitude is much greater than s_C , t_s.

- The transition time, t_{trz}, marks the moment when $\beta_t \Delta T > \beta_c \Delta C$ [1]:

$$t_{trz} \sim L^2 \cdot \left(N^2 D\right)^{-1}, \qquad (24)$$

where the buoyancy ratio is $N = \beta_c \Gamma_w L / \left(\beta_t \Delta T\right)$.

If the equilibrium time at an abscissa is greater than t_{trz}, then, the MDC regime replaces the HDC regime at that x co-ordinate.

- The second moment of interest – the time when $\partial C/\partial x$ becomes greater than s_C – is established considering the equation (23) and it takes the following form:

$$t_s \sim \frac{{s_C}^2 x^2}{{\Gamma_w}^2 D} \qquad (25)$$

If the equilibrium time of the concentration field is smaller than t_s, then $\partial C/\partial x$ is of order of magnitude of the environment, s_C. I will call this situation "case s_C". Otherwise, the $\partial C/\partial x$ term is greater than s_C, a situation called "case $\partial C/\partial x$".

3.2. The heat driven convection (HDC) regime analysis

For the $Pr = \nu/\alpha > 1$ and $Le = \alpha/D \geq 1$ case, the scientific literature [5] indicates an amplitude of the vertical velocity:

$$v_T \sim \frac{g\beta_t \left(\delta_{ech,T}\right)^2_T}{\nu} \gamma^2 \Delta T, \qquad (26)$$

where $\gamma = 1 - \left(1 + Pr^{1/2}\right)^{-1}$. In this case, the velocity boundary layer thickness is $\delta_v = (Pr)^{1/2} \delta_T$. The equilibrium is reached when the horizontally diffused heat flux has the same order of magnitude as the vertically convected heat flux: $v_T \cdot \frac{\partial T}{\partial x} \sim \alpha \cdot \frac{\partial^2 T}{\partial y^2}$.

Using the equations (22) and (26), the equilibrium time is [1] $\left(t_{ech,T}\right)_T \sim \frac{L^2}{\alpha}\left(\frac{X}{Ra \cdot \gamma^2 \cdot Gr^{1/4}}\right)^{1/2}$ or

$$\left(\tau_{ech,T}\right)_T \sim \left(\frac{X \cdot Gr^{5/4}}{Ra \cdot \gamma^2}\right)^{1/2} \qquad (27)$$

The concentration field in the HDC regime. For the analysed case, the order of magnitude of the velocity in the concentration field is $\left(v_C\right)_T = v_T \frac{\delta_C}{\delta_T}$. The relative magnitude of the $\partial C/\partial x$ and the s_C terms defines two situations:

a) "case $\partial C/\partial x$". The scale analysis requires:

$$v_T \frac{\delta_C}{\delta_T} \cdot \frac{\partial C}{\partial x} \sim D \frac{\partial^2 C}{\partial y^2} \qquad (28)$$

Using the equations (23), (26), and (27), the equilibrium time of the concentration boundary layer thickness is [1]

$$\left(t_{ech,C}\right)_T \sim \frac{L^2}{D}\left(\frac{X}{Ra \cdot \gamma^2 \cdot Le^{4/3} \cdot Gr^{1/4}}\right)^{1/2} \text{ or}$$

$$\left(\tau_{ech,C}\right)_T \sim \left(\frac{X \cdot Le^{2/3} \cdot Gr^{5/4}}{Ra \cdot \gamma^2}\right)^{1/2} \qquad (29)$$

The equilibrium time, $\left(t_{ech,C}\right)_T$, is bigger than the transition time, t_{trz}, if:

$$X > X_{trz,C} = Ra \cdot \gamma^2 \cdot Le^{4/3} \cdot N^{-4} \cdot Gr^{1/4} \qquad (30)$$

b) "case s_C". At the limit, $\partial C/\partial x$ has the order of magnitude of s_C and the scale analysis reveals that

$$v_T \frac{\delta_C}{\delta_T} \cdot s_c \sim D\left(\frac{\partial^2 C}{\partial y^2}\right) \qquad (31)$$

Using (23), (26) and (27), the equilibrium time becomes:

$$\left(t_{ech,Sc}\right)_T \sim \frac{L^2}{\alpha} \frac{1}{S_C}\left[Gr^{1/4} / \left(X \cdot Ra^3 \cdot \gamma^6\right)\right]^{1/4} \qquad (32)$$

The equilibrium time $\left(t_{ech,,Sc}\right)_T$ will be compared, further, to t_{trz} and t_s :

b1) the equilibrium time $\left(t_{ech,,Sc}\right)_T$ is smaller than the transition time, t_{trz}, if:

$$X > N^8 \cdot Gr^{1/4} \cdot \left(Ra^3 \cdot \gamma^6 \cdot {S_C}^4 \cdot Le^4\right)^{-1} = X_{trz,Sc} \qquad (33)$$

b2) the possibility to have $\left(t_{ech,Sc}\right)_T < t_s$ defines the following domain:

$$X > Gr^{1/4} \cdot \left(Ra \cdot \gamma^2 \cdot Le^{4/3} \cdot {S_C}^4\right)^{-1/3} = X_{S,T} \qquad (34)$$

Similarly [1], two distinct situations appear (see fig. 2):

1. If the equation (35) is true, then $X_{trz,Sc} < X_{S,T} < X_{trz,C}$ and a HDC regime attains the equilibrium state along the entire wall (fig. 2 (a)).

$$M = Ra \cdot \gamma^2 \cdot S_C \cdot Le^{4/3} \cdot N^{-3} \geq 1 \qquad (35)$$

2. If $Ra \cdot \gamma^2 \cdot S_C \cdot Le^{4/3} N^{-3} < 1$, then: $X_{trz,C} < X_{S,C} < X_{trz,Sc}$; a HDC_C region is encountered on the $[0, X_{trz,C}]$ domain, while a MDC regime is encountered beyond $X_{trz,C}$ abscissa (fig. 2(b)).

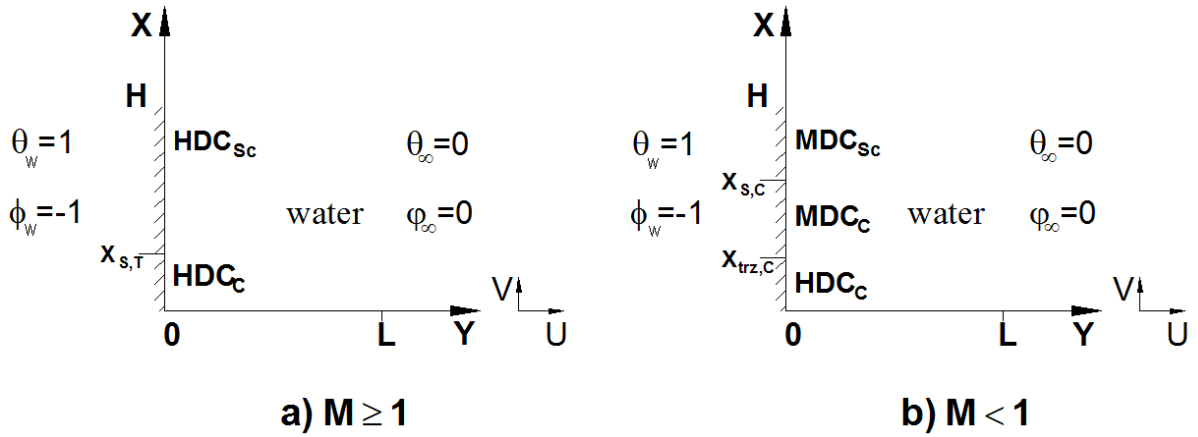

Fig. 2. *The heat and mass driven natural convection regimes sequence. (a) $M \geq 1$; (b) $M < 1$*

3.3. Scale analysis of the mass driven convection (MDC) analysis

Using a similar analysis, the vertical velocity scale in the MDC regime is:

$$v_C \sim \frac{g\beta_c (\delta_{ech,C})^2 C}{\nu} \lambda^2 \Delta C, \qquad (36)$$

where $\lambda = 1 - (1 + Sch^{1/2})^{-1}$; here, Sch is the Smith number, $Sch = \nu \cdot D^{-1}$. The velocity boundary layer thickness is $\delta_v = (Sch)^{1/2} \delta_C$. The **MDC**$_{Sc}$ regime (where the $\partial C/\partial x$ term is of the order of magnitude of s_c) and **MDC**$_C$ regime (the $\partial C/\partial x$ term is much greater than s_c) are presented separately by fig. 2(b).

MDC$_{Sc}$ regime. The equilibrium between the horizontal diffusion and the vertical convection of the mass is written: $v_C \cdot s_c \sim D\left(\frac{\partial^2 C}{\partial y^2}\right)$. Using equation (36), the equilibrium time is [1] $(t_{ech,Sc})_c \sim \frac{L^2}{D}\left(\frac{1}{N \cdot Ra \cdot \lambda^2 \cdot S_C \cdot Le}\right)^{1/2}$ or

$$(\tau_{ech,Sc})_c \sim Gr^{3/4} \cdot \left(\frac{Le}{N \cdot Ra \cdot \lambda^2 \cdot S_C}\right)^{1/2} \qquad (37)$$

The inequality $(t_{ech,Sc})_C < t_s$ or

$$X > \left(Pr \cdot \lambda^2 \cdot N \cdot S_C{}^5 \cdot Le\right)^{-1/4} = X_{S,C} \qquad (38)$$

defines the X co-ordinate that separates the MDC$_C$ and the MDC$_{Sc}$ regimes in fig. 2(b).

4 PERTURBATION FIELD

The perturbation field is defined by equation (39), where the "B" subscript refers to the base values and the "~" superscript refer to the perturbation values. The governing equations (40-43) with the boundary conditions (44-47) are solved using the finite differences method [1-3].

$$V = V_B + \tilde{V};\ U = U_B + \tilde{U};\ P = P_B + \tilde{P};\ \theta = \theta_B + \tilde{\theta};\ \varphi = \varphi_B + \tilde{\varphi};\ \zeta = \zeta_B + \tilde{\zeta};\ \Psi = \Psi_B + \tilde{\Psi}. \qquad (39)$$

$$\tilde{\zeta} = \left(\frac{\partial^2 \tilde{\Psi}}{\partial Y^2} + \frac{\partial^2 \tilde{\Psi}}{\partial X^2}\right) \qquad (40)$$

$$\frac{\partial \tilde{\zeta}}{\partial \tau} + U_B \frac{\partial \tilde{\zeta}}{\partial Y} + \tilde{U} \frac{\partial \zeta_B}{\partial Y} + V_B \frac{\partial \tilde{\zeta}}{\partial X} + \tilde{V} \frac{\partial \tilde{\zeta}}{\partial X} = \frac{Pr}{Gr^{1/4}} \cdot \left(\frac{\partial^2 \tilde{\zeta}}{\partial Y^2} + \frac{\partial^2 \tilde{\zeta}}{\partial X^2}\right) + \frac{Pr^2}{Gr^{1/4}} \cdot \left(\frac{\partial \tilde{\theta}}{\partial Y} + N \frac{\partial \tilde{\varphi}}{\partial Y}\right); \qquad (41)$$

$$\frac{\partial\tilde{\theta}}{\partial\tau}+U_B\frac{\partial\tilde{\theta}}{\partial Y}+\tilde{U}\frac{\partial\theta_B}{\partial Y}+V_B\frac{\partial\tilde{\theta}}{\partial X}+\tilde{V}\frac{\partial\theta_B}{\partial X}= \\ =\frac{1}{Gr^{1/4}}\left(\frac{\partial^2\tilde{\theta}}{\partial Y^2}+\frac{\partial^2\tilde{\theta}}{\partial X^2}\right); \quad (42)$$

$$\frac{\partial\tilde{\varphi}}{\partial\tau}+U_B\frac{\partial\tilde{\varphi}}{\partial Y}+\tilde{U}\frac{\partial\varphi_B}{\partial Y}+V_B\frac{\partial\tilde{\varphi}}{\partial X}+\tilde{V}\frac{\partial\varphi_B}{\partial X}+ \\ +\tilde{V}S_C\frac{1}{Gr^{1/4}}=\frac{1}{LeGr^{1/4}}\left(\frac{\partial^2\tilde{\varphi}}{\partial Y^2}+\frac{\partial^2\tilde{\varphi}}{\partial X^2}\right). \quad (43)$$

$$\tilde{\Psi}=\frac{\partial\tilde{\Psi}}{\partial Y}=0,\ \tilde{\varphi}=\tilde{\theta}=0 \text{ at } Y=0 \quad (44)$$

$$\frac{\partial\tilde{\Psi}}{\partial Y}=0,\ \tilde{\zeta}=0,\ \tilde{\theta}=\tilde{\varphi}=0 \text{ as } Y=L; \quad (45)$$

$$\tilde{\Psi}=0,\ \tilde{\zeta}=0,\ \tilde{\theta}=\tilde{\varphi}=0 \text{ at } X=0; \quad (46)$$

$$\frac{\partial^2\tilde{\psi}}{\partial X^2}=\frac{\partial^3\tilde{\psi}}{\partial X^3}=\frac{\partial^2\tilde{\theta}}{\partial X^2}=\frac{\partial^2\tilde{\varphi}}{\partial X^2}=0 \text{ at } X=H \quad (47)$$

5. RESULTS AND DISCUSSIONS

Figure 3 presents the temperature (fig 3.(a)), the concentration (fig. 3(b)), the stream function ((fig. 3(c)), and the $\partial\varphi/\partial X$ (fig. 3(d)) graphs of the case I. Analyzing fig. 3, we notice:

1. $N\cdot\Delta\varphi<\Delta\theta$ along the wall which indicates that a heat driven convection regime is installed along the entire wall.
2. $\partial\varphi/\partial X>0.0$ for $X<3.46$, while (34) indicates us a value of 3.7352 for $X_{S,T}$. The two values are considered to be very close.

Figure 4 presents the results of the finite difference modeling of the second case. The temperature field (Fig. 4(a)), the $N\cdot\varphi$ field (Fig. 4(b)), the stream function (Fig. 4(c)), and the $\partial\varphi/\partial X$ field (Fig. 4(d)) show us the following important aspects:

1. the scale analysis indicates us the abscissa that separates the HDC and the MDC regime $(N\cdot\Delta\varphi\cong\Delta\theta=1)$ as being $X_{trz,C}\approx 1.91$. At this abscissa, Fig. 4(b) shows a value of $N\cdot\varphi\cong 1.06$. It is a good agreement of the results.
2. the $X_{S,C}$ abscissa that separates the MDC_c and the MDC_{Sc} regimes is defined by (38). It gives us a value of $X_{S,C}\cong 3.69$, while fig. 4(d) indicates us a value of $X\cong 3.5$ (where $\partial\varphi/\partial X\cong 3.0\times10^{-6}$).

Figures 3 and 4 verify the correct choice of the two parameter sets for the illustration of the HDC and the HDC-MDC regimes situation.

Further, instantaneous temperature perturbations of a magnitude $A=8.0$ will be applied to the base fields. For the first case, fig. 5 presents the temperature (fig. 5(a, d)), the concentration (fig. 5(b, e)), and the vertical velocity (fig. 5(c, f)) perturbation fields for two moments ($\tau=15$ and $\tau=48$). The perturbation was applied at $X=1.5$.

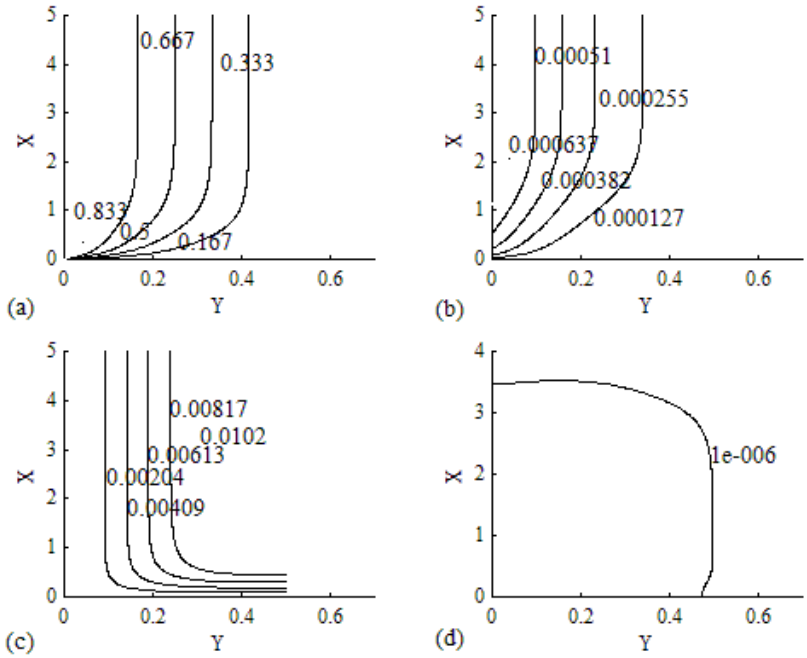

Fig. 3. *The temperature (a), the concentration (b), the stream function (c) and the* $\partial\varphi/\partial X$ *(d) graphs for* $Ra=1.0\times10^{11}$, $N=1$, $Le=2$, $Pr=6.7$, $S_C=0.05$

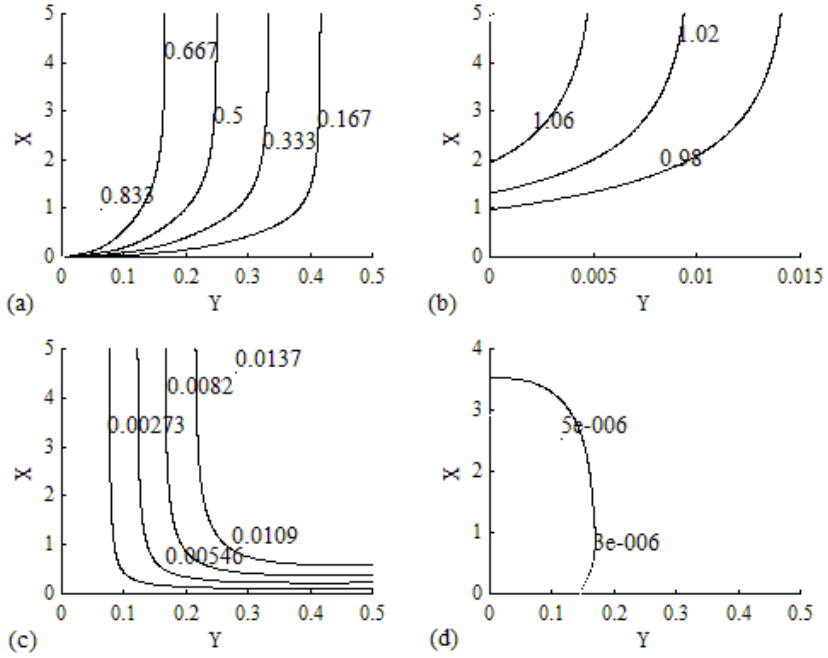

Fig. 4. *The temperature (a), the concentration (b), the stream function (c) and the* $\partial\varphi / \partial X$ *(d) graphs for* $Ra = 1.0 \times 10^{11}$, $N = 3000$, $Le = 1$, $Pr = 6.7$, $S_C = 0.04$

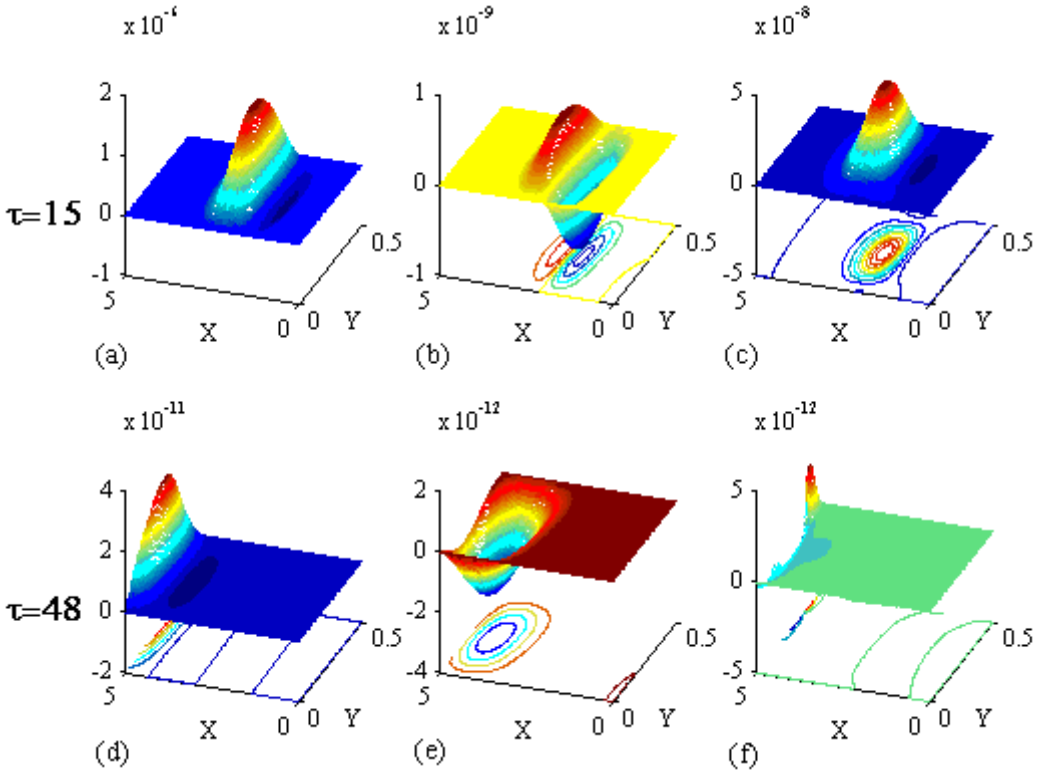

Fig. 5. *The perturbation temperature (a, d), concentration (b, e), vertical velocity fields (c, f) for* $Ra = 1.0 \times 10^{11}$, $N = 1$, $Le = 2$, $Pr = 6.7$, $S_C = 0.05$

We notice that the perturbation moves to the higher abscissas, while its magnitude diminishes, a characteristic of the convective instability. Similar results are obtained for temperature perturbations applied at other abscissas along the wall.

Figure 6 presents the perturbation fields for the second case, the HDC-MDC regime succession. The temperature (fig. 6(a, d, g)), concentration (fig. 5(b, e, h)), and vertical velocity (fig. 5(c, f, i)) perturbation fields are presented for three moments ($\tau = 45$, $\tau = 65$ and $\tau = 75$). If it is applied at $X = 1.5$ (in the HDC region), the perturbation moves upwards

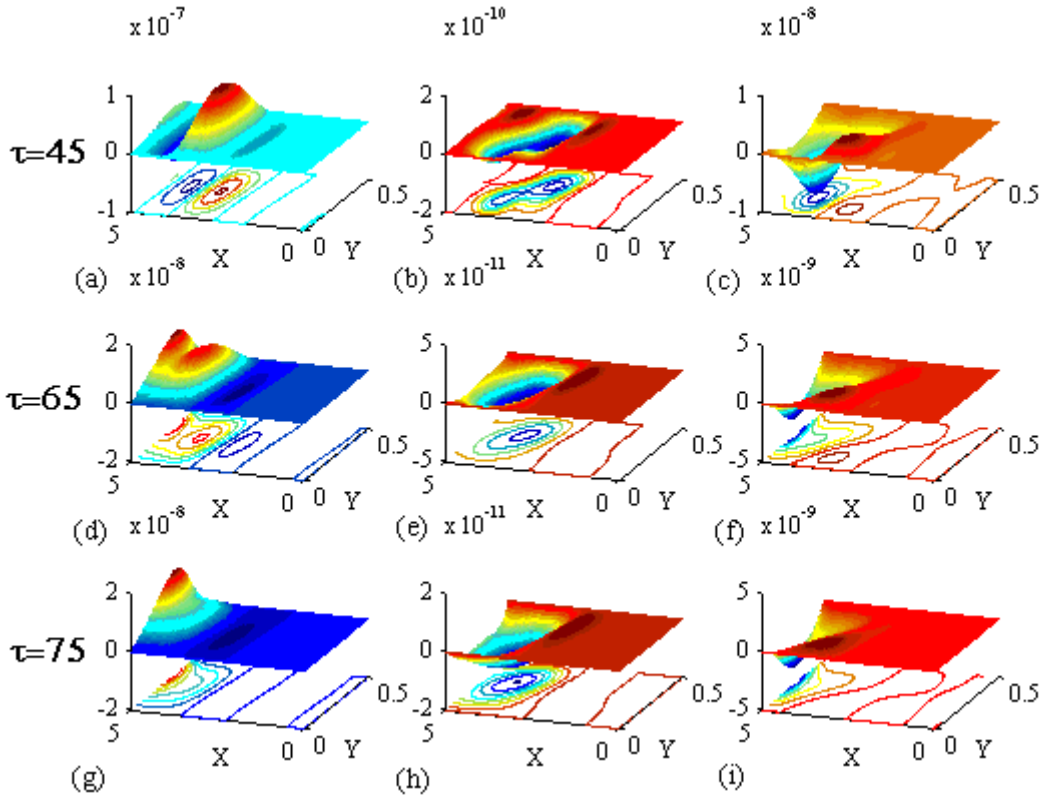

Fig. 6. *The perturbation temperature (a), the concentration (b), vertical velocity fields for* $Ra = 1.0 \times 10^{11}$, $N = 3000$, $Le = 1$, $Pr = 6.7$, $S_C = 0.04$

decreasing its amplitude. After arriving at the upper limit (fig. 2(d)-(f)), the perturbation gains a negative vertical velocity and moves towards the starting point, a mark of an absolute unstable convection case.

If the perturbation is applied at the $X = 2.0$ abscissa (in the MDC region) a convectively unstable regime is registered, similar to the case analyzed by fig. 5.

We should make a comparison with the results of Tao ([6]) even if we are analyzing here a double diffusive convection. They show a convectively unstable regime for the constant flux boundary and a region of absolute instability for the constant temperature boundary case. The Rayleigh number $Ra = 1.0 \times 10^{11}$ is situated in the absolute instability region of the constant temperature boundary case.

CONCLUSIONS

This paper analyses the natural convection process near a vertical impermeable wall of constant temperature and mass flux. The wall is situated in a mass stratified environment. Two possibilities appear as a function of the process parameters: a heat-driven convection (HDC) regime along the wall or a HDC-MDC (mass-driven convection) regimes succession.

The analysis performed using two particular parameter sets for a Rayleigh number of 1.0×10^{11} shows that the two type of regime convection have a great influence on the stability of the system:

- the HDC regime is convectively unstable no matter where the perturbation is applied along the wall;
- the HDC-MDC regime is convectively unstable if the perturbation is applied in the MDC region and it is absolutely unstable if it is applied in the HDC region.

These results strengthen the importance of the natural convection regime type and they suggest the necessity for further analysis.

REFERENCES

[1] Neagu, M., *Natural convection near a vertical wall of constant mass flux and temperature situated in a mass stratified fluid*, IOP Conference Series: Materials Science and Engineering, 444, 2018, pag. 1-14;

[2] Neagu, M., *Heat/mass driven natural convection of air near a boundary of constant mass flux and temperature*, Journal of Multidisciplinary Engineering Science and Technology, 8, 2021, pag. 14727-14735;

[3] Neagu, M., *The succession of heat and mass driven natural convection regimes along a vertical impermeable wall*, European Journal of Natural Sciences and Medicine, 5, 2022, pag. 9-26;

[4] Neagu, M., *The stability analysis of a linearly mass stratified fluid near a vertical impermeable wall of a constant temperature and mass flux*, Journal of Multidisciplinary Engineering Science and Technology, 10, 2023, pag. 15804-15811;

[5] Patterson, J.C., Lei, C., Armfield, S.W. and Lin, W., *Scaling of unsteady natural convection boundary layers with a non-instantaneous initiation*, International Journal of Thermal Sciences, 48, 2009, pag. 1843-1852;

[6] Tao, J., *Spatio-temporal instability of the natural-convection boundary layer in the thermally stratified medium*, Journal of Fluid Mechanics, 518, 2004, pag. 363-379.